

HELIOSEISMOLOGY, SOLAR MODELS AND NEUTRINO FLUXES

V. Castellani^a, S. Degl'Innocenti^b, W.A. Dziembowski^c, G. Fiorentini^d and B. Ricci^e

^aDipartimento di Fisica dell'Università di Pisa, piazza Torricelli 1, I-56100 Pisa, Italy
and Istituto Nazionale di Fisica Nucleare, LNGS, I-67010 Assergi (L'Aquila), Italy

^bDipartimento di Fisica dell'Università di Pisa, piazza Torricelli 1, I-56100 Pisa, Italy
and Istituto Nazionale di Fisica Nucleare, Sezione di Ferrara, Via Paradiso 12, I-44100 Ferrara, Italy

^cCopernicus Astronomical Center, ul. Bartycka 18, P-00716 Warsaw, Poland

^dDipartimento di Fisica dell'Università di Ferrara, I-44100 Ferrara
and Istituto Nazionale di Fisica Nucleare, Sezione di Ferrara, Via Paradiso 12, I-44100 Ferrara, Italy

^eIstituto Nazionale di Fisica Nucleare, Sezione di Ferrara, Via Paradiso 12, I-44100 Ferrara, Italy

We present our results concerning a systematical analysis of helioseismic implications on solar structure and neutrino production. We find $Y_{ph} = 0.238 - 0.259$, $R_b/R_\odot = 0.708 - 0.714$ and $\rho_b = (0.185 - 0.199) \text{ gr/cm}^3$. In the interval $0.2 < R/R_\odot < 0.65$, the quantity $U = P/\rho$ is determined with an accuracy of $\pm 5^\circ/\circ$ or better. At the solar center still one has remarkable accuracy, $\Delta U/U < 4\%$. We compare the predictions of recent solar models (standard and non-standard) with the helioseismic results. By constructing helioseismically constrained solar models, the central solar temperature is found to be $T = 1.58 \times 10^7 \text{ K}$ with a conservatively estimated accuracy of 1.4%, so that the major uncertainty on neutrino fluxes is due to nuclear cross section and not to solar inputs.

1. Introduction

Helioseismology allows us to look into the deep interior of the Sun, probably more efficiently than with neutrinos. The highly precise measurements of frequencies and the tremendous number of measured lines enable us to extract the values of sound speed inside the sun with accuracy better than 1%. Recently it was demonstrated that a comparable accuracy can be obtained for the inner core of the Sun [1].

The present work summarizes the results of our group in the last year concerning a systematic analysis of helioseismic implications on solar structure and neutrino production.

We quantitatively estimated the accuracy of solar structure properties as inferred from the measured frequencies through the so called inversion method. This analysis provided the base for quantitative tests of solar models. These tests are briefly presented here, see [1-3] for more details.

Concerning the organization of the paper, af-

ter a short introduction to helioseismic data and their interpretation (sect. 2), we shall discuss the accuracy of solar properties as deduced from helioseismology (sect. 3).

Next (sect. 4) we shall confront with helioseismology the predictions of Standard Solar Models (SSMs). These tests are really a big success of recent SSMs, *including* elements diffusion, so that one can gain further confidence in the predicted central solar temperature and T_c and neutrino fluxes Φ_i .

However, one can take a somehow different attitude. The richness of helioseismic data can be used so as to supply information on some of the less certain inputs of solar models (*e.g.* solar opacity). This is the approach we shall pursue to build Helioseismically Constrained Solar Models (HCSMs), to be discussed in sect. 5.

From the analysis of HCSMs it comes out that T_c can be predicted with an accuracy of about one percent, a result obtained even if some of the most

controversial assumptions of SSM are released.

This result contradicts recently advocated non-standard solar models, build so as to significantly decrease T_c . Actually we show explicitly that these models are in conflict with helioseismic data, see sects. 6 and 7.

Future prospects and applications of helioseismology are presented in sect. 8.

2. Helioseismic data and their interpretation

Traditional and still most important helioseismic observables are frequencies of normal modes of solar oscillations. This is unlike in geophysical seismic sounding where the primary data are travel times of seismic waves. A possibility of measuring the wave travel times in the Sun has been discovered not long ago [4]. The travel time data have been successfully applied to probing subsurface flows [5,6]. The possibility of sounding short lived phenomena localized in the subsurface layers is the advantage over the sounding based on the frequency data. Here, however, we are interested in sounding mean and solar structure and therefore we will not discuss further this new method.

The frequencies of solar oscillations are deduced from time series of the intensity or radial velocity data. The latter are much more frequently used. Long-time continuous monitoring is essential for precise frequency determination. Four ground-based networks of automatic telescopes devoted to helioseismic observations are currently operated. The BISON [7] and IRIS [8] networks measure radial velocity variations for the unresolved solar images. With this method, only modes of low spherical harmonic degrees ($\ell \leq 3$) are detectable. The GONG [9] and TON [10] networks use imaging instruments allowing to detect modes up to $\ell \approx 250$ and $\ell \approx 700$, respectively. There are three seismic instruments on the board of the SOHO spacecraft which started operation at the beginning of 1996. The GOLF [11] instrument is similar to that used by IRIS. The LOI instrument [12], which measures intensity variation, has a capability for detecting modes with $\ell \leq 8$. The third is MDI, which an imag-

ing instrument [13]. In the continuous mode of operation it detects modes up to $\ell = 250$.

Data for seismic probing from the imaging instruments are usually provided in the form of centroid frequencies, $\nu_{\ell n}$, and splitting coefficients, $a_{k\ell n}$, for the ℓ, n multiplets, where n denotes radial order of the mode. The coefficients describe the azimuthal dependence in oscillation frequencies according to the following relation

$$\nu_{\ell nm} = \nu_{\ell n0} + \sum_{k=1} a_{k\ell n} \mathcal{P}_k(m),$$

where subscripts n and m denote radial and azimuthal orders, respectively, and functions $\mathcal{P}_k(m)$ are k -order orthogonal polynomials. Data from the GONG network and from the MDI instrument provide values of $\nu_{\ell n0}$ and six a_k coefficients for over 2000 (ℓn) multiplets. For smaller number of multiplets the coefficients up to $k = 36$ are available in the data sets from the MDI instrument.

Values of a_k 's reveal that the interior rotation rate is not very different from the surface rate and that the Sun is a very slowly rotating and almost perfectly spherical star. This fact significantly simplifies interpretation of the data. In particular, the quantities $\nu_{\ell n0}$, $a_{2k+1, \ell n}$, and $a_{2k, \ell n}$ are separate probes of, respectively, the radial structure, the differential rotation and the asphericity. The possibility of sounding internal rotation is of great importance for understanding mechanism of the solar magnetic activity changing in the 11-year cycle. The data reveal that the differential rotation observed in the surface persists through the convective zone (some outer 30% in the radius). The transition to essentially uniform rotation takes place in the narrow zone, which has been the suggested site of the solar dynamo [14]. An important result in the context of this review is that there is no evidence for the rotation increase toward the center. In fact, according to some studies (e.g. [15]) there is a seismic evidence for lower rotation rate in the core than in outer layers. In any case the dynamical effect of centrifugal force is certainly negligible. There is also no evidence for a significant role of magnetic field in the Sun's interior.

We now focus on the centroid frequencies and,

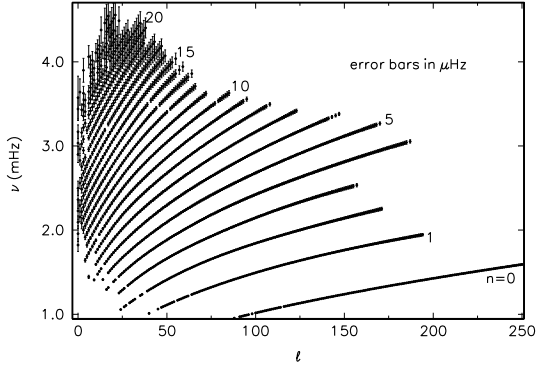


Figure 1. Frequencies of solar oscillations determined from 360-day measurements with the MDI/SOHO instrument. The error bars have been magnified by factor 1000.

as an example, on the data from the MDI/SOHO instrument. The frequencies with the error bars are shown in Fig. 1. The accuracy, which at the low frequencies is $\sim 10^{-5}$, visibly deteriorates at higher frequencies. The peaks in this part of the oscillation amplitude spectra are considerably broader, which is connected with the shorter lifetime of the higher frequency modes. The total number of frequency data in the figure is 2047. The $n = 0$ branch represents fundamental modes which are horizontally propagating waves obeying the same dispersion as surface waves in deep water. Their frequencies are fully determined by mean density in the Sun. The $n \geq 1$ branches represent p-modes which are standing acoustic (pressure) waves. These waves begin their downward propagation from the surface, where they are reflected, as nearly vertical rays. As a result of increasing adiabatic sound speed (a), the rays become gradually more oblique and, eventually, are reflected at the surface where the sound speed satisfies the condition $a(R)/R = 2\pi\nu/\sqrt{\ell(\ell+1)}$.

Only a small fraction of p-modes from Fig. 1 penetrates the energy producing core. At $\nu \approx 3$ mHz and $\ell = 1$, the inner reflection surface occurs at $R = 0.06R_{\odot}$, which is close to the maximum the differential ^8B -neutrino flux of and well beneath the maximum of the differential photon flux. However, at a similar frequency and $\ell = 5$ the reflection takes place at $R = 0.18R_{\odot}$, where the photon flux is already more than 92%

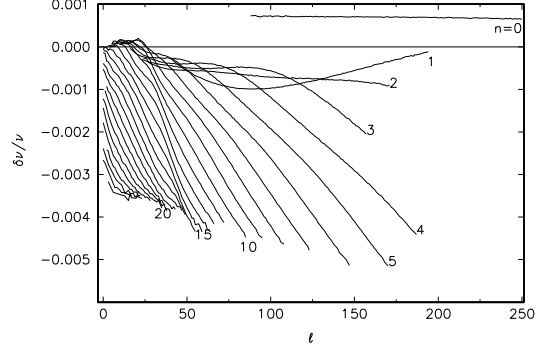


Figure 2. Relative differences between solar (shown in Fig. 1) and frequencies calculated for standard solar model, “model S” of Ref. [30].

of the total solar luminosity. Even for the low degree modes the frequencies are mainly sensitive to the structure of the outer layers. The modes which are very sensitive to the core structure are g-modes. Their frequencies, however, are below 0.43 mHz and we may only hope that the solar g-modes will be some times detected.

In Fig. 2 we show the relative differences in frequency between the Sun and one of the standard solar models. Similar patterns are found for other models. The differences are small in the sense that there is no ambiguity in assigning the n value. However, they exceed the measurement errors frequently by two orders of magnitude. Thus, they are very significant and must be explained. In the case of the f-modes almost all the difference may be removed by an adjustment of the model radius [16]. Solar seismic radius is by 0.045% less than adopted in the model. For higher order p-modes the difference between model and solar frequencies rapidly increases with ℓ . This immediately suggests that most of the difference between the model and the Sun must be localized in outermost layers. Higher ℓ implies a higher R at the lower reflecting surface and therefore a greater confinement to outer layers.

We know that our treatment of the structure and oscillations in outer layers is inadequate. The problem is how to take into account effects of vigorous and nonadiabatic convection. We expect the problem concerns the layers above $R = 0.99R_{\odot}$, where p-modes propagate almost verti-

cally and the local properties are ℓ -independent. This implies that the part of the frequency difference may be modeled in the form $F(\nu)/I$, where I is the calculated mode inertia assuming uniform normalization and F should be determined from the data. It is found that for modern standard solar models this part dominates in $\delta\nu$ but we are interested only in the small contribution arising in the rest of the interior.

In the deeper layers the neglect of dynamical effects of convection is fully justified. Furthermore, the nonadiabatic effects in oscillations, which have not been taken into account in calculation of frequencies used in Fig. 2, are certainly negligible below $R = 0.99R_\odot$. In view of the small values of $\delta\nu/\nu$, linearization about the reference standard model seems justified. Thus, we may use the variational principle for adiabatic stellar oscillations to connect the frequency difference to the differences in structural functions between the Sun and its model. Our aim is to determine these differences. In general, we have to consider simultaneously two unknown functions of R . For one the choices are differences in density, ρ , pressure P , or any combination of them or their derivatives. All such functions are linked by linearized hydrostatic condition. We use here $U = P/\rho$. For the other thermodynamic function the choices are the adiabatic exponent $\Gamma_1 = (\partial \ln P / \partial \ln \rho)_{\text{ad}}$ or squared adiabatic sound speed, $a^2 = U\Gamma_1$. The problem is simplified if we make use the $\Gamma_1(P, \rho, Y)$ relation, where Y is the fractional helium abundance, from the astrophysical equation of state data. (see e.g. Ref. [16]). Since in the chemically inhomogeneous interior we may safely neglect $\delta\Gamma_1$, the problem may be reduced to determination of the function $\delta U(R)$ and the number δY_{ph} – the abundance of He in the layers above the base of the convective zone. In this way the basic equation for seismic probing of the internal structure becomes:

$$\left(\frac{\delta\nu}{\nu}\right)_j = \int \mathcal{K}_j \frac{\delta U}{U} dR + \mathcal{J}_j \delta Y_{ph} + \frac{F(\nu)}{I_j}, \quad (1)$$

where $j \equiv (n, \ell)$. The kernel \mathcal{K}_j and numbers \mathcal{J}_j , I_j are easily evaluated in terms of the eigenfunctions for adiabatic oscillations in the standard solar model.

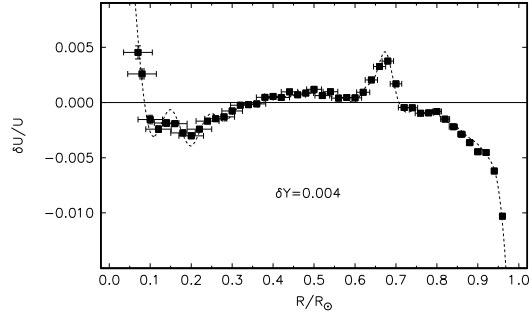


Figure 3. Relative differences in $U = p/\rho$ between the Sun and the model inferred from the differences in ν shown in Fig. 2. The symbols with error bars give the averaged values with the Gaussian-like localized kernels. The horizontal error bars give the full width at half-maxima of the kernels. Vertical error bars directly reflect the observational errors. The dashed line represents the result of inversion by means of the regularized least square method in which $\delta U/U$ is searched in the form of a superposition of cubic splines. Near the center results obtained with this method are unreliable. The value of $\delta Y_{ph} = (4.0 \pm 0.1) \times 10^{-3}$ was determined simultaneously with $\delta U/U$.

This equation may be applied to all p-modes. Thus, we have a large set of the integral equations to determine the two functions and the Y_{ph} . Methods of determination of $\delta U/U$ were described in details in Refs. [17] and [18]. There are two distinct approaches. The first is the regularized least squares (RLS) method which consists in a discretization in terms of known function and a determination of parameters by means of minimization of the χ -squared fit plus an integral term that smooths artificial oscillation. The other is the optimal averaging method which consists in seeking linear combination of individual kernels which are close to possibly narrow Gaussians centered at specified distances R . Corresponding combination of frequency differences yields the averaged values of $\delta U/U$ weighted with these localized kernels. Fig. 3 shows that the results obtained with these methods agree in a good agreement.

Once we know $\delta U(R)$ we may determine $\delta\rho(R)$, $\delta P(R)$ and δM_R making no additional assump-

tions. Hence we get seismic values of these three parameters in the whole solar interior. At this stage we can determine the value R at the base of the convective, R_b , as well as the temperature $T(R)$ for $R \geq R_b$. What we cannot find is $T(R)$ $Y(R)$ profiles in the radiative interior. In order to disentangle the two last functions, which are of course most interesting in the context of the solar neutrino problem, we have to use data on the opacities and the nuclear reaction rates. This has been done (see Ref. [17] for references to the original work) but we will not pursue this way here. Rather, we rely on directly inferred quantities as constraints on solar models.

We see in Fig. 3 that the relative differences in U are less than 5×10^{-3} in the whole $[0.05 - 0.95]R_\odot$ range of R . This agreement is very unlikely accidental and, thus, we regard it as a confirmation of the standard model of the solar evolution. In the outer part of the convective zone the agreement is worse but it may be easily improved by admissible modifications in the description of the convective energy transfer. Beneath $R = 0.05R_\odot$ we just do not have enough information to make any statement. The small differences in the intermediate region may be eliminated by introducing *ad hoc* opacity modifications which are within the uncertainty of its calculation [19]. However, the bump in $\delta U/U$ near the bottom of the convective envelope may have another cause. Richard et al. [20] showed that this feature may be removed if one allows a weak rotation-induced mixing of elements below the bottom of the convective envelope. The effect was considered as a possible explanation of the deficiency of lithium in the Sun's atmosphere. Mixing brings lithium to deeper layers where it burns. It also results in a reduction efficiency of the gravitational settling leading to somewhat higher Y_{ph} in the convective zone. Thus, the same effect may also explain the seismic correction to the photospheric He abundance ($\delta Y_{ph} = 4 \times 10^{-3}$).

3. How accurate are solar properties as inferred from helioseismology?

We performed a systematic and possibly exhaustive investigation of the uncertainties of the

helioseismic approach, in order to estimate the global error to be assigned to helioseismic determinations of solar properties. With this spirit, we analyse several physical quantities Q characterizing the solar structure. Concerning the outer part of the sun, we discuss the photospheric helium abundance Y_{ph} , the depth of the convective envelope R_b , and the density at the bottom of the convective zone ρ_b . Then we consider the “intermediate” solar interior ($x=R/R_\odot = 0.2 - 0.65$), analysing the behaviour of the squared isothermal sound speed, $U=P/\rho$. Finally we investigate the inner region ($x \leq 0.2$), where nuclear energy and neutrinos are produced.

We remind –see the previous section– that helioseismology measures *only* the frequencies $\{\nu\}$ of solar p-modes, and quantities characterizing the solar structure are indirectly inferred from the $\{\nu\}$'s, through an inversion method. Schematically, the procedure is the following:

a) One starts with a solar model, giving values Q_{mod} and predicting a set $\{\nu_{mod}\}$ of frequencies. These will be somehow different from the measured frequencies, $\nu_\odot \pm \Delta\nu_\odot$

b) One then searches for the corrections δQ to the solar model which are needed in order to match the corresponding frequencies $\{\nu_{mod} + \delta\nu\}$ with the observed frequencies $\{\nu_\odot\}$. Expression for $\delta\nu$ are derived by using perturbation theory, where the starting model is used as a zero-th order approximation. The correction factors δQ are then computed, assuming some regularity properties, so that the problem is mathematically well defined and/or unphysical solutions are avoided.

c) The “helioseismic value” Q_\odot is thus determined by adding the starting value and the correction ¹:

$$Q_\odot = Q_{mod} + \delta Q. \quad (2)$$

For each quantity Q we have determined the partial errors corresponding to each uncertainties of the helioseismic method. In fact, there are three independent sources of errors in the inversion process:

¹ Concerning notation, we remark that δQ indicates the correction to solar model to obtain helioseismic value (see Eq. 2), whereas ΔQ indicates the estimated uncertainty on Q .

Table 1

For the indicated quantities Q we present the helioseismic values Q_\odot and the relative errors $\Delta Q/Q$. All uncertainties are in $^\circ/\infty$. In the fifth and sixth row, for $U = P/\rho$ the values of the uncertainties are the maxima in the indicated interval. In the last two rows the results on U at points representative of the ${}^7\text{Be}$ and ${}^8\text{B}$ neutrino production are shown.

Q	Q_\odot	$\left(\frac{\Delta Q}{Q}\right)$
Y_{ph}	0.249	42
R_b/R_\odot	0.711	4
ρ_b [g/cm ³]	0.192	37
$U(0.2 < x < 0.65)$		5
$U(0.1 < x < 0.2)$		9.4
$U(x_{Be})$ [10^{15} cm ² s ⁻²]	1.56	17
$U(x_B)$ [10^{15} cm ² s ⁻²]	1.56	22

i) Errors on the measured frequencies, which – for a given inversion procedure – propagate on the value of Q_\odot .

ii) Residual dependence on the starting model: the resulting Q_\odot is slightly different if one starts with different solar models. This introduces an additional uncertainty, which can be evaluated by comparing the results of several calculations.

iii) Uncertainty in the regularization procedure. Essentially this is a problem of extrapolation/parametrization. Different methods, equally acceptable in principle, yield (slightly) different values of Q_\odot .

It has to be remarked that, in view of the extreme precision of the measured frequencies, $\Delta\nu_\odot/\nu_\odot \lesssim 10^{-4}$ [21–24], uncertainties corresponding to ii) and iii) are extremely important.

For deriving a global uncertainty, we took a very conservative approach. Maybe that the parameter variation was not exhaustive, and what we found as extrema are not really so, but actually are quite acceptable values. In view of this, let us double the interval we found and interpret $\pm(\Delta Q)_k$, as partial errors. Furthermore, let us be really *conservative* assuming that errors add up linearly. In conclusion, this gives:

$$\Delta Q = \pm \sum_k |(\Delta Q)_k|. \quad (3)$$

In the following sections, we shall use this error estimate.

3.1. Properties of the convective envelope

Three independent physical properties of the convective envelope are determined most accurately by seismic observations, see Ref.[1]: Y_{ph} , R_b and ρ_b ².

The helioseismic predictions, together with their (conservatively estimated) accuracy, are shown in Table 1. We remark that for all these quantities the uncertainty resulting from propagation of the frequency measurement errors is of minor importance with respect to the “systematic” errors, intrinsic to the inversion method.

3.2. The intermediate region

The essential output of helioseismology is the reconstruction of the adiabatic sound speed profile, a . Our discussion is in terms of the related quantity U ; as well known (see also sect. 2), $a^2 = \Gamma_1 U$ and Γ_1 is given by the equation of state with an accuracy of 10^{-3} or better (even the simplest EOS, fully ionized perfect classical gas yields $\Gamma_1 = 5/3$ with an accuracy of about 10^{-3}).

By using the RLS method (see sect. 2) it is possible to derive directly the profile of U as a function of the radial coordinate throughout all the sun, except for the inner region ($x < 0.1$). The results (values of U and global errors), are summarized in Table 1.

²A fourth seismic “observable”, the sound speed at the convective radius is traditionally considered, e.g. [25]. We have not included it in our list since, as shown in Ref.[26], it is not an independent one.

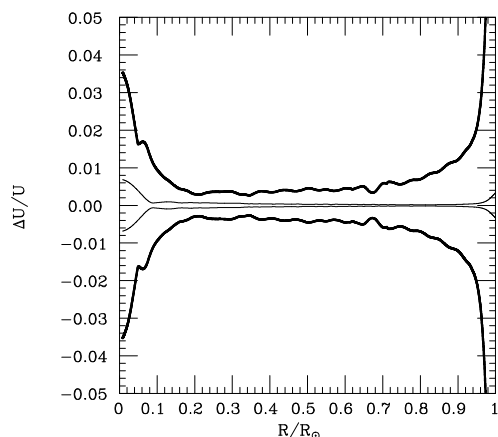


Figure 4. The estimated global relative uncertainty on $U = P/\rho$ (thick line) and that due to the observational errors (thin line).

It is convenient to consider an intermediate solar region: $0.2 < x < 0.65$. The upper limit is established by requiring that it is well below the transition to the convective zone, which we discussed above. The lower limit is chosen so as to exclude the region of energy production (see next subsection). For this region the following comments are relevant:

a) Each of the individual uncertainties nowhere exceeds $2^\circ/\infty$.

b) Uncertainties from the accuracy on the measured frequencies are of minor relevance with respect to the residual model dependence and to the sensitivity to the inversion parameters, see Fig. 4.

c) All in all, even with the most conservative estimates, the helioseismic determination is extremely accurate: $|\Delta U/U| \leq 5^\circ/\infty$ throughout the explored region.

3.3. The energy production region

As well known, most of the energy and of solar neutrinos originate from the innermost part of the sun. According to SSM calculations, see e.g. Refs. [27,28], about 94% of the solar luminosity and 93% of the pp neutrinos are produced within $x < 0.2$, the region which we analyse in this section.

Our results are summarized in Fig. 4 and Table 1. Clearly the precision worsens in this region, due to the fact that p-modes do not penetrate in

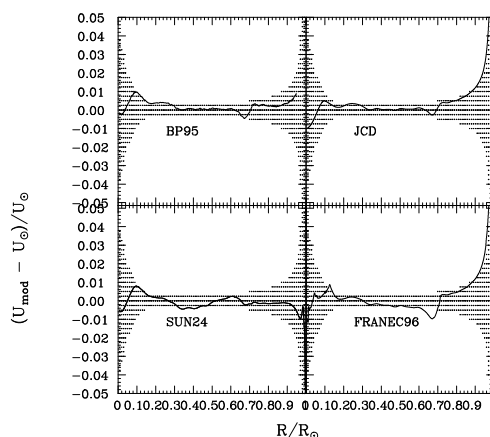


Figure 5. The difference between U as predicted by selected solar models, U_{mod} , and the helioseismic determination, U_{\odot} , normalized to this latter. The dotted area corresponding to $(\frac{\Delta U}{U})$. SUN24 is the “model 0” of Ref. [17]; FRANEC96 is the “best” model with He and heavier elements diffusion of Ref. [29]; BP95 is the model with metal and He diffusion of Ref. [28]; JCD is the “model S” of Ref. [30].

the solar core, and consequently the information one can extract from available experimental results is limited, but still important.

For example, at the production maxima of ${}^7\text{Be}$ and ${}^8\text{B}$ neutrinos ($x_{Be} = 0.06$ and $x_B = 0.04$ according to our best solar model with diffusion [29]) the global accuracy is still a 2%, see Table 1. Even at $x = 0$ the accuracy is 3.5%. In conclusion, *helioseismology provides significant insight even on the solar innermost core.*

4. Helioseismology and SSMs

The comparison between the predictions of a few recent SSM calculations and helioseismic information is shown in Figs. 5 and 6.

Concerning the (isothermal) sound speed profile, see Fig. 5, all models look generally good. Also SUN24, a model which neglects elemental diffusion, passes this test.

The study of convective envelope is illuminating, see Fig. 6. All models neglecting elemental diffusion are in clear contradiction with helioseismic constraint. On the other hand, calculations where diffusion is included look in substan-

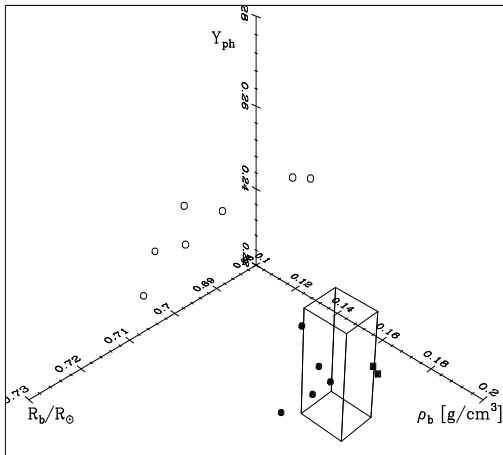


Figure 6. Helioseismic determinations and solar model predictions of properties of the convective envelope. The box defines the region allowed by helioseismology. Open circles denote models without diffusion, squares models with He diffusion, full circles models with He and heavier elements diffusion, see Ref. [1].

tial agreement with helioseismology.

All this shows that the two approaches (profile of U and properties of the convective envelope) are complementary and both important.

The previous arguments show that SSMs are in good shape. Actually, helioseismology provides a new perspective/definition of SSMs.

Before the advent of helioseismology a SSM had three essentially free parameters, α , Y_{in} and $(Z/X)_{in}$ for producing three measured quantities: the present radius, luminosity and heavy element content of the photosphere. This may not look as a too big accomplishment, in itself.

Nowadays, by using the same number of parameters a SSM has to reproduce many additional data, such as Y_{ph} , R_b , ρ_b , $U(R)$, provided by helioseismology.

Alternative solar models have to be confronted with these data too.

5. Helioseismically constrained solar models

Helioseismic data are thus in agreement with recent SSM calculations, which use accurate equations of state, recent opacity tables and include helium and heavier elements diffusion

[31,1,28–30], see also Ref. [20]. These SSMs yield central temperatures $T_{c,SSM}$ which differ from each other by not more than 1%. However the uncertainties in the input parameters, mainly the opacity κ and the heavy elements abundance Z/X , result in $(\Delta T_c/T_c)_{SSM} \approx 1 - 2\%$.

From helioseismic observations one cannot determine directly temperatures of the solar interior, as one cannot determine the temperature of a gas from the knowledge of the sound speed unless the chemical composition is known. However, it is possible to obtain the range of allowed values of the central temperature T_c , by selecting those solar models which are consistent with seismic data.

Our calculations are not model-independent, but we shall use in principle a wider class of models in comparison with SSMs, which we call helioseismically-constrained solar models (HCSM). These models are based on the same equilibrium and evolution equations as SSMs, but they differ in the choice of some input parameters. We generate this class of models by using the FRANEC code [29] for the SSMs and varying the input parameters. Each choice of the set of parameters gives some value of T_c .

We obtain the range of allowed values of T_c by selecting those solar models which are consistent with seismic data. More specifically, we shall determine the central temperature $T_{c,HCSM}$, as that of the model which gives the best fit to the seismic data and the uncertainties, $\Delta T_{c,HCSM}$, corresponding to the range spanned by models consistent with these data.

We remind that the precise value of the temperature is governed essentially by two quantities: the radiative opacity κ and the fraction of heavy elements Z/X . As well known the uncertainties on κ and Z/X are of the order of 10%. Furthermore, these uncertainties do not correspond to clear experimental or observational errors, rather they are determined by judicious comparison among published values. As an example, the uncertainty on κ can only be estimated from the comparison among recent theoretical calculations.

We allowed that both κ and Z/X are rescaled by free multiplicative factors with respect to the value used in the SSM. These scaling factors are

Table 2

Predictions of neutrino fluxes and signals in the Cl and Ga detectors from HCSMs. Uncertainties corresponding to $(\Delta T/T)_{HCSM} = \pm 1.4\%$ are shown (first error) together with those from nuclear cross sections (second error).

Φ_{Be}	$[10^9/\text{cm}^2/\text{s}]$	$4.81 \pm 0.53 \pm 0.59$
Φ_B	$[10^6/\text{cm}^2/\text{s}]$	$5.96 \pm 1.49 \pm 1.93$
Cl	[SNU]	$8.4 \pm 1.9 \pm 2.2$
Ga	[SNU]	$133 \pm 11 \pm 8$

then determined by helioseismic constraints on the convective envelope.

In this way (see Ref. [32]), we obtained as the best estimate $T_{HCSM} = 1.58 \times 10^7$ K, with a conservatively estimated uncertainty $(\Delta T/T)_{HCSM} = \pm 1.4\%$, to be compared with the uncertainty of SSM calculations $(\Delta T/T)_{SSM} = \pm 2.7\%$.

We remark the following points:

i) The “best” temperatures determined by means of helioseismology starting from different solar models converge.

ii) The uncertainty $(\Delta T_c)_{HCSM}$ is (slightly) reduced with respect to $(\Delta T_c)_{SSM}$.

iii) More important, the helioseismic uncertainty is related to observational data (whereas as noted above $\Delta\kappa$, and thus $(\Delta T_c)_{SSM}$, was derived just from comparison among theoretical calculations).

Let us come over to *neutrino fluxes*, Φ_i ($i = \text{pp}, {}^7\text{Be}, {}^8\text{B}$). Their dependence on the central temperature T_c is parametrized as:

$$\Phi_i = \Phi_{i,SSM} \left(\frac{T_c}{T_{c,SSM}} \right)^{\beta_i}. \quad (4)$$

From numerical experiments with FRANEC, we found: $\beta_{pp} = -0.92$, $\beta_{Be} = 7.9$, $\beta_B = 18$.

We have determined neutrino fluxes by starting with different SSMs, renormalizing their predictions to the same temperature $T_{HCSM} = 1.58 \cdot 10^7$ K and to the same (updated) nuclear cross sections. The resulting fluxes and signals, all very close to each other, have been averaged to determine the HCSM predictions shown in Table 2, where the first error corresponds to a conservatively estimate $(\Delta T_c/T_c)_{HCSM} = 1.4\%$. and the second one to a 3σ error on nuclear cross sections.

We remark that nuclear physics uncertainties look larger than astrophysical ones. After the successful LUNA experiment measuring the

${}^3\text{He}+{}^3\text{He}$ cross section [33], the main uncertainties arise now from the astrophysical S-factor for ${}^3\text{He}+{}^4\text{He}$ and $\text{p}+{}^7\text{Be}$ reactions, which should be measured more accurately.

6. A mixed solar core?

Several authors have proposed non-standard solar models, where some ad-hoc mechanism is introduced, so as to reduce the central solar temperature by a few percent, which might alleviate (not solve) the solar neutrino puzzle.

Clearly such a reduction of T_c is in contrast with the conclusions of the previous section. Here we show explicitly that such models are inconsistent with helioseismic information.

As an example, consider the case of a mixed solar core, firstly advanced by Shaviv and Salpeter in 1968 [34] and recently revived by Haxton and Cumming [35], see also Refs. [28,36]. Roughly speaking, mixing of H and He over an *appreciable* portion of the sun enriches the innermost solar core with H. Hydrogen burning becomes more efficient and the solar luminosity is attained at lower core temperatures. This results in reduced T_c , ${}^7\text{Be}+\text{CNO}$ and ${}^8\text{B}$ neutrino fluxes, again if a significant portion ($R > 0.1R_\odot$) of the Sun is mixed.

Several different mixing processes (fast or slow, continuous or episodic) can be conceived [37,34, 38–41]. While we refer to Ref. [3] for an extended discussion, we concentrate here on the case of fast continuous mixing.

In Fig. 7 we show (dashed line) the relative difference between the isothermal sound speed squared, $U = P/\rho$, as predicted by the mixed models and the helioseismic determination, U_\odot . The same quantity for our SSM is also shown

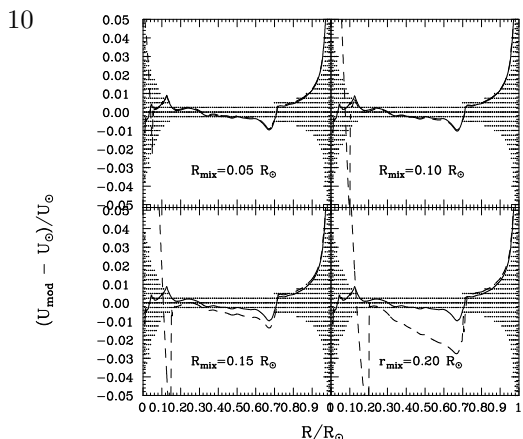


Figure 7. For the indicated values of R_{mix} , we present the relative difference between the isothermal sound speed as predicted by solar model with fast continuous mixing, U_{mod} , and the helioseismic determination, U_{\odot} (dashed lines). The same quantity for our SSM is also shown (solid line). The dotted area corresponds to the uncertainty on U_{\odot} .

(solid line).

One sees a strong deviation of Mixed Core Models (MCMs), with respect to both U_{\odot} and U_{SSM} , in the mixing zone; this is a consequence of the change in “mean molecular weight”, μ , induced by mixing. In the approximation of perfect gas (accurate to the level of few per thousand in the solar core) one has $U \propto T/\mu$. Due to mixing, the innermost region is enriched with hydrogen, so that μ decreases (we observe that change of μ can be as high as 40%, whereas temperature change is at most a few per cent) and U increases. The opposite occurs near the edge of the mixed region.

As the mixing area increases, the sound speed profile of the MCMs deviates more and more from the SSM prediction and it becomes in conflict with helioseismic constraint if $R_{mix} \geq 0.1R_{\odot}$.

Neutrino fluxes predicted by MCMs are shown in Fig. 8. One sees that reduction of intermediate (${}^7\text{Be}+\text{CNO}$) and/or high (${}^8\text{B}$) energy neutrino fluxes is only achieved for $R_{mix} \geq 0.1R_{\odot}$.

Similar conclusions hold for the other mixing mechanisms mentioned above, see Ref. [3].

In brief, *reduction of ${}^7\text{Be}$ and ${}^8\text{B}$ neutrino fluxes can only be obtained for extended mixing*

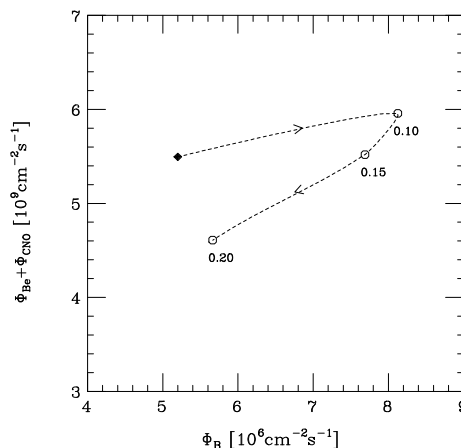


Figure 8. The predictions of intermediate (${}^7\text{Be}+\text{CNO}$) and high energy (${}^8\text{B}$) neutrino fluxes in solar models with continuous fast mixing, for the indicated values of R_{mix} . The prediction of our SSM (full diamond) is also shown.

regions ($R_{mix} \geq 0.1R_{\odot}$), corresponding to solar models inconsistent with helioseismic constraints.

We remind that the one percent accuracy of helioseismic information at $R/R_{\odot} \approx 0.1$ is an essential ingredient for achieving this result.

7. Helioseismology and physics of fundamental interactions

As another example illustrating the potential of the helioseismic approach we discuss the $\text{p}+\text{p} \rightarrow \text{d}+\text{e}^++\nu_e$ reaction.

The rate of the initial reaction in the pp chain is too low to be directly measured in the laboratory (even in the solar center this rate is extremely small, clearly of the order of 10^{-10} yr^{-1}) and it can be determined only by using the theory of low energy weak interactions, together with the measured properties of the deuteron and of the proton-proton scattering. While we refer to Refs. [42,43,27] for updated reviews, we remind that, as input of SSM calculations, one takes [43] $S_{pp,SSM} = 3.89 \cdot 10^{-25} (1 \pm 0.01) \text{ MeV b}$.

We remark however that only theoretical estimates of S_{pp} are available and observational information would be welcome. In this respect, it is interesting to determine the range of S_{pp} which is acceptable in comparison with helioseismology.

In sect. 5 we pointed that there are two major

uncertainties in building SSMs: solar opacity κ and heavy element abundance $\zeta = Z/X$ are only known with an accuracy of about $\pm 10\%$. By using now κ , ζ and as S_{pp} free parameters, we can determine the acceptable range of S_{pp} by requiring that R_b , ρ_b and Y_{ph} are all predicted within the helioseismic range. The dependence of these quantities on κ , ζ and S_{pp} has been determined numerically in Ref. [32].

Most of the information on S_{pp} arises from data on ρ_b as this observable depends strongly on S_{pp} whereas it is weakly affected by the others parameters. One can understand the dependence on S_{pp} , at least qualitatively. A value of S_{pp} larger than $S_{pp,SSM}$ implies smaller temperatures in the solar interior, which thus becomes more opaque (in other words, the region of partial ionization is deeper). Radiative transport therefore is less efficient and convection starts deeper in the Sun ($R_b < R_{b,SSM}$), where density is higher ($\rho_b > \rho_{b,SSM}$).

By restricting to the allowed ranges for the properties of the convective envelope, see Table 1, also taking into account the predictions of different SSMs, we find:

$$0.94 \leq S/S_{SSM} \leq 1.18 \quad (5)$$

In conclusion, we remark that helioseismology provides the only observational constraint, although indirect, on the $p+p \rightarrow d + e^+ + \nu_e$ reaction.

Incidentally, we observe that this analysis completely excludes the value $S_{pp} = 2.9S_{pp,SSM}$, recently found in Ref. [44], by using a too rough description of the low energy pp scattering data, see also Ref. [45].

8. Future prospects and further applications

The helioseismic observation of the Sun will continue and the accuracy of the frequency data will improve. For solar physicists most hope is connected with the possibility of studying changes during the coming maximum of the magnetic activity. Astronomers interested in the angular evolution are looking forward to new data which should tell us whether indeed solar core

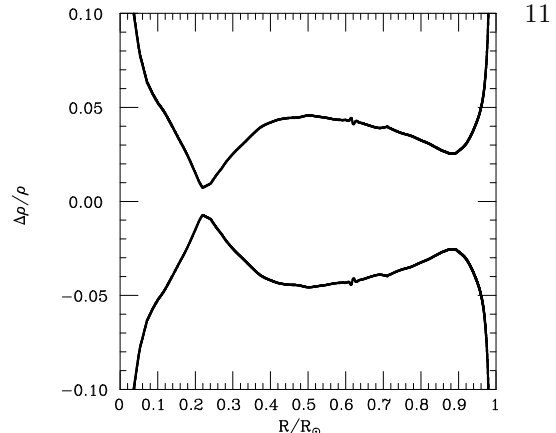


Figure 9. The estimated global relative uncertainty on ρ .

rotates slower than the outer layers. This is so strange that most of them hesitate to believe it now.

We do not expect revelations as far as internal structure is concerned. The chances to find something that would shake the standard model of stellar evolution seem very small. Unquestionably, however, there is a room for improvement and helioseismology may help.

As a few examples of relevance to calculation of precise solar models for evaluation of the neutrino fluxes as well to modeling evolution of other stars, we briefly outline a few topics we are presently working on.

8.1. The solar density profile

From the knowledge of $U = P/\rho$ along the solar profile, by using the hydrostatic equilibrium equation, one can extract the solar density (see *e.g.* [18]). We performed a systematic analysis of the uncertainties so as to provide a quantitative estimate of the accuracy $\Delta\rho/\rho$, the preliminary result being presented in Fig. 9.

We remark that accurate predictions of the solar density, are important for determining the $\nu_e \rightarrow \nu_x$ transition probability in neutrino oscillation models where neutrino conversion is due to matter effects, see *e.g.* [46–48].

8.2. Solar opacity

As remarked above, solar opacity $\kappa(R)$ is the more uncertain *ingredient* of solar models. By

using the additional information provided by helioseismology one can try to transform it into an *output* of frequencies measurements. The idea is as follows: as we know $U = P/\rho$, we have one more information on solar structure, and we can use one of the equations of stellar equilibrium/evolution for getting κ .

In fact, in the region beyond the energy producing core and below the convective envelope ($0.2 < R/R_\odot < 0.65$) one can use the radiative transport equation in the form:

$$\kappa(R)\rho(R) = \frac{-16\pi\sigma}{3L_\odot} \frac{dT^4}{dR} R^2 \quad (6)$$

where L_\odot is the solar luminosity. In the same region the perfect gas equation (for fully ionized H and He and for neutral Z) holds to high accuracy and the (almost) uniform abundance of He and Z can be inferred from the observed properties of the solar photosphere. In this way temperature gradients can be expressed in terms of gradients of U (again determined from helioseismology) so that the photon mean free path, $\lambda = 1/(\kappa\rho)$, can be extracted, possibly with a few per cent accuracy.

This could provide an observational, although indirect, test of opacity calculation for plasma condition as in the solar interior, see also Ref. [49].

8.3. The statistical distribution of nuclei in the solar core

Already two decades ago, Kacharov *et.al.* [50] and Clayton *et.al.* [51], speculated that the high energy tail of the distribution of protons in the solar core could depart from the Maxwell exponential form,

$$\frac{dN_{Max}(E)}{dE} \rightarrow \frac{dN_{Max}}{dE} \exp[-\delta(E/KT)^2] \quad (7)$$

as an attempt to reduce the prediction of ^8B neutrino flux by invoking a depletion in the number of protons with energy high enough to be captured by ^7Be nuclei.

Recently interest in this matter was revived by Quarati *et.al.* [52], who provided some argument for such a depletion, in the frame of non extensive Tsallis statistics.

In fact, sub barrier nuclear reaction provide a good laboratory for testing the high energy tail of the distribution, as they involve particles near the Gamow peak E_G , which is generally larger than the average thermal energy KT . Tiny deviation from the Maxwellian distribution, undetectable near KT , would be amplified at higher energies, see Eq. 7.

If the energy distribution deviates from the Maxwellian form, the reaction rates $\langle\sigma v\rangle$ would differ from those calculated with the Maxwell distribution

Clearly this also holds for the basic $p+p \rightarrow e^+ + \nu_e$ reaction. As we discussed in sect. 7, its rate can be constrained by helioseismology. In the same way, possible deviations from the Maxwell distribution can be studied, see Ref. [53]

We are grateful to Venja Berezhinsky for a friendly collaboration during the last few years. We thank the director of Osservatorio Astronomico di Collurania, Teramo, and the director of Laboratori Nazionali del Gran Sasso for their hospitality.

REFERENCES

1. S. Degl'Innocenti, W.A. Dziembowski, G. Fiorentini and B. Ricci, *Astrop. Phys.* 7 (1997) 77.
2. S. Degl'Innocenti, G. Fiorentini and B. Ricci, *astro-ph/9707133*, to appear on *Phys. Lett. B* (1997).
3. S. Degl'Innocenti and B. Ricci, *astro-ph/9710292*, 1997.
4. T.L.Jr. Duvall, S.M. Jefferies, J.W. Harvey, M.A. Pomerantz, *Nature* 362 (1993) 430.
5. T.L. Duvall Jr., S. D'Silva, S.M. Jefferies, J.W. Harvey, J. Schou, *Nature* 379 (1996) 235.
6. A.G. Kosovichev, *Ap. J. Lett.* 461 (1996) 55.
7. Y. Elsworth, R. Howe, G.R. Isaak, C.P. McLeod, B.A. Miller, H.B. Van der Raay, R.J. Wheeler, in *GONG'94: Helio- and Astero-Seismology*, R.K. Ulrich, E.J. Rhodes Jr. and Däppen (eds.) ASP Conference Series, Vol.

- 76, p.392, 1995.
8. E. Fossat, in *GONG'94: Helio- and Astreo-Seismology*, R.K. Ulrich, E.J. Rhodes Jr. and Däppen (eds.) ASP Conference Series, Vol. 76, p.387, 1995.
 9. J. Leibacher, and The Gong Project Team, in *GONG'94: Helio- and Astreo-Seismology*, R.K. Ulrich, E.J. Rhodes Jr. and Däppen (eds.) ASP Conference Series, Vol. 76, p.381, 1995.
 10. D.Y. Chou, K.R. Chen and TON Team, *Bull. Astr. Soc. India* 24 (1996) 133.
 11. A.H. Gabriel *et.al.*, *Solar Phys.*162 (1995) 61.
 12. C. Frölich *et.al.*, *Solar Phys.*162 (1995) 101.
 13. P.H. Scherrer *et.al.*, *Solar Phys.*162 (1995)129.
 14. P.A. Gilman, C.A. Morrow, E.E. DeLuca, *Ap. J.* 338 (1989) 528.
 15. T. Rabello Soares, T. Roca Cortés, A. Jiménez, T. Appourchaux, A. Eff-Darwich, *Ap. J.* 480 (1997) 840.
 16. J. Schou, A.G. Kosovichev, P.R. Goode, W.A. Dziembowski, *Ap. J. Lett.* (1997) to appear.
 17. W.A. Dziembowski, *Bull. Astr. Soc. India* 24 (1996) 133.
 18. W.A. Dziembowski, P.R. Goode, A.A. Pamyatnykh and R. Sienkiewicz, *Ap. J.* 432 (1994) 417.
 19. S.C. Tripathy, S Basu, J. Christensen-Dalsgaard, in *Proc. IAU Symp. 181: Sounding Solar and Stellar Interior*, F.X. Schmider and J. Provost (eds.), 1997, in press
 20. O. Richard, S. Vauclair, C. Charbonnel and W.A. Dziembowski, *Astr. Astroph.* 312 (1996) 1000.
 21. K.G. Libbrecht, M.F. Woodard and J.M. Kaufman, *Ap. J. Suppl.* 74 (1990) 1129. F.P. Pijpers and M.J. Thompson, *Astron. Astr.* 262 (1992) L33.
 22. Y. Elsworth, R. Howe, G. Isaak and C.P. McLeod, R. New, *Ap. J.* 434, (1994) 801.
 23. S. Tomczyk, K. Ständer, G. Card, D. Elmore, H. Hull and A. Cacciani, *Sol. Phys.* 159 (1995) 1.
 24. J.E. Harvey *et.al.*, *Science*, 272 (1996) 1284.
 25. J. Christensen-Dalsgaard, *Nucl. Phys. B (Proc. Suppl.)* 48 (1996) 325.
 26. J. Christensen-Dalsgaard, D.O. Gough and M.J. Thompson *Ap. J.* 378 (1991) 413.
 27. V. Castellani, S. Degl'Innocenti, G. Fiorentini, M. Lissia and B. Ricci, *Phys. Rep* 281 (1997) 309.
 28. J.N. Bahcall and M.H. Pinsonneault, *Rev. Mod. Phys* 67 (1995) 781.
 29. S. Degl' Innocenti, F. Ciaccio and B. Ricci, *Astr. Astroph. Suppl. Ser.* 123 (1997) 1.
 30. J. Christensen-Dalsgaard *et.al.* , *Science* 272 (1996) 1286.
 31. J.N. Bahcall and M.H. Pinsonneault, S. Basu and J. Christensen-Dalsgaard, *Phys. Rev. Lett.* 78 (1997) 171; J.N. Bahcall, S. Basu and P. Kumar, *ApJ. Lett.* (1997) to appear.
 32. B. Ricci, V. Berezinski, S. Degl'Innocenti, W.A. Dziembowski and G. Fiorentini, *Phys. Lett. B* 407 (1997) 155.
 33. C. Arpesella *et.al.*, *Phys. Lett. B* 389 (1997) 452
 34. G. Shaviv and E. Salpeter, *Phys. Rev. Lett.* 21 (1968) 1602.
 35. A. Cumming and W.C. Haxton, *Phys. Rev. Lett.* 77 (1997) 4286.
 36. O. Richard and S. Vauclair, *Astr. Astroph.* 322 (1996) 671.
 37. D. Ezer and A.G.W. Cameron, *Ap. J. Lett.* 1 (1968) 177.
 38. J.N. Bahcall, N.A. Bahcall and R.K. Ulrich, *Ap. J. Lett.* 2 (1968) 91.
 39. G. Shaviv and E.E. Salpeter, *Ap. J.* 165 (1971) 171.
 40. R.K. Ulrich and E.J. Rhodes, *Ap. J.* 265 (1983) 551.
 41. R. Sienkiewicz, J.N. Bahcall and B. Paczynski, *Ap. J.* 349 (1990) 641.
 42. J.N. Bahcall and M.H. Pinsonneault, *Rev. Mod. Phys.* 64 (1992) 885.
 43. M. Kamionkowski and J.N. Bahcall, *Ap. J.* 420 (1994) 884.
 44. H. Oberhummer *et.al.*, *astro-ph/9705119* (1997); H. Oberhummer *et.al.*, *astro-ph/9705046* (1997).
 45. J.N. Bahcall and M. Kamionkowski, *astro-ph/9707320*, to appear on *Nucl. Phys. A* (1997)
 46. P.I. Krastev and A.Yu. Smirnov, *Phys. Lett. B* 226 (1989) 341.
 47. H. Nunokawa, A. Rossi, V.B. Semikov and

- J.W.F. Valle, Nucl. Phys. B 472 (1996) 495.
48. P. Bamert, C.P. Burgess and D. Michaud, hep-ph/9707542 (1997).
 49. J.R. Elliott, Month.Not.Roy.Astron.Soc. 277 (1995) 1567.
 50. S. Vasil'ev, G. Kocharov and A. Levkovskii, Ser. Fiz. 38 (1974) 1827; S. Vasil'ev, G. Kocharov and A. Levkovskii, Ser. Fiz. 39 (1975) 310.
 51. D.D. Clayton, Nature 249 (1974) 131; D.D. Clayton, E. Eliahu, M.J. Newman and R.J. Talbon, Ap. J. 199 (1975) 494.
 52. P. Quarati, A. Carbone, G. Gervino, G. Kanadiakis, A. Lavagno and E. Miraldi, Nucl. Phys. A 621 (1997) 345; G. Kanadiakis, A. Lavagno and P. Quarati, Phys. Lett. B 369 (1996) 308; G. Kanadiakis and P. Quarati, Physica A 192 (1993) 677.
 53. Lissia *et.al.*, in preparation.